TUM

Kernel Embedding for Particle Gibbs-Based Optimal Control

Scientific thesis for the procurance of the degree M.Sc.
(Intermediate report)
from the TUM School of Computation, Information and Technology
at the Technical University of Munich.

Supervised by	Univ.-Prof. Dr.-Ing. Sandra Hirche M.Sc. Robert Lefringhausen Chair of Information-Oriented Control
Submitted by	cand. ing. Lukas Hochschwarzer l.hochschwarzer@gmail.com
Submitted on	Munich, XX.XX.2024

April 26, 2024

M A S T E R ' S   T H E S I S
for
Lukas Sebastian Hochschwarzer
Degree Electrical Engineering and Information Technology

Kernel Embedding for Particle Gibbs-Based Optimal Control

Problem description:

Bayesian learning-based control approaches are promising for safety-critical systems where physical modeling is time-consuming or impossible. A common problem in such systems is that not all states can be measured, resulting in the absence of a closed-form expression for the posterior distribution. However, particle Markov chain Monte Carlo (PMCMC) methods like particle Gibbs sampling can draw samples from the posterior distribution. These samples can be used to formulate a scenario optimal control problem (OCP), for whose solution probabilistic constraint satisfaction guarantees can be inferred [1]. However, representing the unknown dynamics using samples is exceedingly inefficient because many samples are required for a good representation. In addition, the scenario OCP must be solved repeatedly to infer probabilistic guarantees.

Kernel embedding is a promising alternative that allows the representation of unknown distributions with few samples, even if their parametric form is unknown. In recent years, this idea has been increasingly used for stochastic optimal control, among others, in [2] and [3]. A major advantage of these approaches is that the desired robustness level can be specified a priori and does not have to be determined by repeatedly solving the OCP.

This thesis thus aims to implement an optimal control approach that combines PMCMC methods for system identification with kernel embedding. Furthermore, the robustness of the proposed approach shall be analyzed, and the resulting algorithm shall be evaluated using simulations.

Tasks:

- Literature research on kernel embedding and PMCMC-based control
- Implementation of an optimal control approach that utilizes kernel embedding
- Robustness analysis of the proposed approach
- Numerical evaluation of the proposed approach

Bibliography:

[1] R. Lefringhausen, S. Srithasan, A. Lederer, and S. Hirche, "Learning-based optimal control with performance guarantees for unknown systems with latent states," *arXiv preprint*, 2023.

[2] J.-J. Zhu, W. Jitkrittum, M. Diehl, and B. Schölkopf, "Kernel distributionally robust optimization: Generalized duality theorem and stochastic approximation," in *International Conference on Artificial Intelligence and Statistics*, pp. 280–288, PMLR, 2021.

[3] A. Thorpe, T. Lew, M. Oishi, and M. Pavone, "Data-driven chance constrained control using kernel distribution embeddings," in *Learning for Dynamics and Control Conference*, pp. 790–802, PMLR, 2022.

Supervisor: M.Sc. Robert Lefringhausen
Start: 06.05.2024
Delivery: 05.11.2024

(S. Hirche)

Abstract

As control engineering methods are applied to increasingly complex systems, data-driven approaches for system identification appear as a promising alternative to physics-based modeling. These approaches, such as particle Markov chain Monte Carlo (PMCMC) methods allow for the joint estimation of uncertain dynamics and latent states in systems where neither is certain or directly measureble. Combining PMCMC methods with scenario theory enables the computation of optimal input trajectories for unknown linear systems with latent states. However, deriving guarantees for these input trajectories is difficult and requires a computationally intentive process.

This paper proposes the use of particle Gibbs sampling in combination with maximum mean discrepancy ambiguity sets as an alternative to scenario theory. This allows for the inclusion of the failure tolerance in the optimization process. The effectiveness of this approach is demonstrated in a numerical simulation.

Contents

Chapter 1

Introduction

Reliable mathmatical models are a fundamental component of any model-based control application. However, finding such a model is often very difficult as there are many considerations that go into creating or estimating it, with even small deviations sometimes leading to big differences. Oftentimes, it is impossible to create such a model only based on the general knowledge of the system, such as the physics of the application. Because of this, data-driven modeling approaches that allow for derive such models based on previously collected data are gaining attention and their usefulness for optimal control applications is being explored.

In this chapter, the problem is introduced in Sec. 1.1 and various works that are connected to this topic are shown and summarized in 1.2.

1.1 Problem Statement

Consider the general nonlinear discrete-time system of the form

$$\boldsymbol{x}_{t+1} = \boldsymbol{f}\left(\boldsymbol{x}_t, \boldsymbol{u}_t\right) + \boldsymbol{v}_t \tag{1.1a}$$

$$\boldsymbol{y}_t = \boldsymbol{g}\left(\boldsymbol{x}_t, \boldsymbol{u}_t\right) + \boldsymbol{w}_t \tag{1.1b}$$

with the state $\boldsymbol{x} \in \mathbb{R}^{n_x \in \mathbb{N}}$, the input $\boldsymbol{u} \in \mathbb{R}^{n_u \in \mathbb{N}}$, the output $\boldsymbol{y} \in \mathbb{R}^{n_y \in \mathbb{N}}$, the process noise $\boldsymbol{v}_t \in \mathbb{R}^{n_x}$, the measurement noise $\boldsymbol{w}_t \in \mathbb{R}^{n_y}$ and time $t \in \mathbb{Z}$.

In our setting, only the output $\boldsymbol{y}$ is observable and the state transition function $\boldsymbol{f}(\cdot)$ and the observation function $\boldsymbol{g}(\cdot)$, as well as the distributions $\boldsymbol{\mathcal{V}}$ and $\boldsymbol{\mathcal{W}}$ of the process noise $\boldsymbol{v}$ and measurement noise $\boldsymbol{w}$ are unknown.

We assume that a dataset $\mathbb{D} = \{\boldsymbol{u}_t, \boldsymbol{y}_t\}_{t=-T:-1}$ containing the last $T \in \mathbb{N}$ measurements of the input $\boldsymbol{u}$ and output $\boldsymbol{y}$ is available.

We further assume that the structure of the model $\{\boldsymbol{f}_{\boldsymbol{\theta}}(\cdot), \boldsymbol{g}_{\boldsymbol{\theta}}(\cdot), \boldsymbol{\mathcal{V}}_{\boldsymbol{\theta}}, \boldsymbol{\mathcal{W}}_{\boldsymbol{\theta}}\}$ is known and is dependent on a finite number of unknown parameters $\boldsymbol{\theta}$. In addition to that, the priors $p(\boldsymbol{\theta})$ and $p(\boldsymbol{x}_{-T})$ are available as well.

The objective is to minimize a given cost function

$$J_H = \sum_{t=0}^{H} c(\boldsymbol{u}_t, \boldsymbol{x}_t, \boldsymbol{y}_t) \tag{1.2}$$

over the horizon H while satisfying the constraints

$$\boldsymbol{h}(\boldsymbol{u}_{0:H}, \boldsymbol{x}_{0:H}, \boldsymbol{y}_{0:H}) \leq \boldsymbol{0} \tag{1.3}$$

with $\boldsymbol{h} \in \mathbb{R}^{n_c}$ being a vector of arbitrary deterministic function. As the states $\boldsymbol{x}_{0:H}$ are unknown to us and there are several uncertain factors in our system, the constraints are transformed into chance-constraints and since it is possible that $\boldsymbol{h}$ is impossible to satisfy for every possible $\boldsymbol{x}_{0:H}$, we also introduce a risk factor $\alpha \in [0, 1]$ that relaxes these constraints, turning them into

$$P\left[h_i(\boldsymbol{u}_{0:H}, \boldsymbol{x}_{0:H}, \boldsymbol{y}_{0:H}) \leq 0\right] \geq 1 - \alpha, \ \forall i = 1, ..., n_c \tag{1.4}$$

with h_i being the i-th element of $\boldsymbol{h}$ and P being generally unknown.

1.2   Related Work

The problem presented in Sec. 1.1 provides several challenges as the information we have available is very limited. While many methods to solve chance constraint problems exist, they often rely on samples from the distribution P which is generally unknown in our problem. While we do have priors for the uncertain elements, samples drawn from this distributions do not allow as to quantify the system enough for practical applications. As such, the priors must be updated based on the input-output measurements $\mathbb{D}$ which generally results in an analytically intractable posterior distribution.

To draw samples from this distribution, methods such as particle Markov chain Monte Carlo (PMCMC) Methods [ADH10] can be used. This has recently been exploited for optimal control in [LSLH24] , utilizing such a sampler to generate scenarios for the system and using these scenarios as a representation of the unknown distribution to formulate a deterministic optimal control problem by reformulating the chance-constraints. However, the usage of the scenarios in this paper comes with the drawback of the risk factor α not being part of the final optimal control problem (OCP) and the process of estimating it retroactively being quite ressource intensive.

As such, there is a need to find other methods that allow us to utilize the samples generated by PG sampler to reformulate the chance-constraints to find a distributionally robust solution without losing the risk factor in the process. As the difficulties with this can be traced back to the unknown distribution P, ambiguity sets have been proposed as a possible workaround. Here, ambiguity sets are defined as a set of probability distributions that are within a certain radius under an appropriate distance function. This was used in [HCL19] with Wasserstein distance

as the metric for the ambiguity set. It has however been proven rather difficult to efficiently construct a Wasserstein ambiguity set for problems.

In contrast, the metric proposed in [NKSZ22] allows for an efficient construction of an ambiguity set using a maximum mean discrepancy (MMD) metric combined with kernel approximation and can be applied to gneral non-linear and non-convex constraints.

The remainder of this paper is structured as follows. In chapter 2, we review the methods used to solve the OCP. These methods are then tested and evaluated in chapter 3 and further discussed in chapter 4. Finally, the results are summarized and some concluding remarks are given in chapter 5.

Chapter 2

Technical Approach

In this chapter, an approach is outlined that allows us to effectively solve the chance-constraint problem defined in section 1.1. In section 2.1 we explain how to draw samples from unknown system and use them to generate scenarios. These scenarios are then used in 2.2 to reformulate and solve the OCP.

2.1 Particle Markov Chain Monte Carlo Methods

For practical applications, the known priors $p(\boldsymbol{\theta})$ and $p(\boldsymbol{x}_{\text{-}T})$ and the observations $\mathbb{D}$ must be used to infer the posterior $p(\boldsymbol{\theta}, \boldsymbol{x}_{\text{-}T:\text{-}1} \mid \mathbb{D})$. This is necessary since the repeated propagation of $p(\boldsymbol{x}_{\text{-}T})$ would otherwise cause an excessively large variance in $p(\boldsymbol{x}_{\text{-}1})$ making stochastic OCP infeasible. We utilize PMCMC methods to draw samples from this distribution. These methods were introduced in [ADH10] and will be summarized in this section.

We use Particle Gibbs (PG) to bypass the issue of an analytically intractable $p(\boldsymbol{\theta}, \boldsymbol{x}_{\text{-}T:\text{-}1} \mid \mathbb{D})$ by iteratively drawing samples from $p(\boldsymbol{\theta} \mid \boldsymbol{x}_{\text{-}T:\text{-}1}, \mathbb{D})$ and $p(\boldsymbol{x}_{\text{-}T:\text{-}1} \mid \boldsymbol{\theta}, \mathbb{D})$. We continually update the distributions with the previously drawn set, i.e. $\boldsymbol{x}_{\text{-}T:\text{-}1}^{[n]}$ is drawn from $p(\boldsymbol{x}_{\text{-}T:\text{-}1}^{[n]} \mid \boldsymbol{\theta}^{[n]}, \mathbb{D})$ and $\boldsymbol{\theta}^{[n+1]}$ is then drawn from $p(\boldsymbol{\theta}^{[n+1]} \mid \boldsymbol{x}_{\text{-}T:\text{-}1}^{[n]}, \mathbb{D})$. This is repeated until the desired number of samples has been achieved. To ensure that the samples drawn through this method are an accurate representation of the distribution $p(\boldsymbol{\theta}, \boldsymbol{x}_{\text{-}T:\text{-}1})$, additional steps are taken. For one, the first N_p samples must be discarded as they are heavily reliant on the initialization and as such might show a strong bias. This burn in period should be chosen large enough so that this bias is no longer reflected in the samples. The samples should also be indepedendent of each other which is not given with this method as each $\boldsymbol{\theta}^{[n]}$ is dependent on $\boldsymbol{x}_{\text{-}T:\text{-}1}^{[n]}$ which in turn is dependent on $\boldsymbol{\theta}^{[n-1]}$. As such, measures must be taken to reduce the correlation between samples as much as possible. One approach to do this is thinning where only every n_d-th sample is used and the other samples are discarded. By increasing this parameter, the samples become more uncorrelated but there will also be a larger amount of samples created which leads to inefficiency.

Algorithm 1 Scenario generation

    Input: Dataset $\mathbb{D}$, parametric model $\{\boldsymbol{f_\theta}(\cdot), \boldsymbol{g_\theta}(\cdot), \boldsymbol{\mathcal{V}_\theta}, \boldsymbol{\mathcal{W}_\theta}\}$,
        priors $p(\boldsymbol{\theta})$ and $p(\boldsymbol{x}_{\text{-}T})$, N, H, T
    Output: Scenarios $\boldsymbol{\delta}^{[1:N]} = \{\boldsymbol{\theta}, \boldsymbol{x}_0, \boldsymbol{v}_{0:H}, \boldsymbol{w}_{0:H}\}^{[1:N]}$

1: **for** $n = 1, \ldots, N$ **do**
2:     Sample $\{\boldsymbol{\theta}, \boldsymbol{x}_{\text{-}T:\text{-}1}\}^{[n]}$ from $p\left(\boldsymbol{\theta}, \boldsymbol{x}_{\text{-}T:\text{-}1} \mid \mathbb{D}\right)$ using a PG sampler
3:     **for** $t = \text{-}1, \ldots, H$ **do**
4:         Sample $\boldsymbol{v}_t^{[n]}$ from $\boldsymbol{\mathcal{V}}_{\boldsymbol{\theta}^{[n]}}$
5:         Sample $\boldsymbol{w}_t^{[n]}$ from $\boldsymbol{\mathcal{W}}_{\boldsymbol{\theta}^{[n]}}$
6:     **end for**
7:     $\boldsymbol{x}_0^{[n]} \leftarrow \boldsymbol{f}_{\boldsymbol{\theta}^{[n]}}\left(\boldsymbol{x}_{\text{-}1}^{[n]}, \boldsymbol{u}_{\text{-}1}\right) + \boldsymbol{v}_{\text{-}1}^{[n]}$
8: **end for**

The samples $\{\boldsymbol{\theta}, \boldsymbol{x}_{\text{-}T:\text{-}1}\}^{[1:N]}$ can be used to generate so-called scenarios $\boldsymbol{\delta}^{[1:N]}$, which are samples from the distribution $p(\boldsymbol{\theta}, \boldsymbol{x}_0, \boldsymbol{v}_{0:H}, \boldsymbol{w}_{0:H} \mid \mathbb{D})$ and represent possible future system behavior depending on $\boldsymbol{u}_{0:H}$. The generation of these scenarios is outlined in Algorithm 1. The parameters $\boldsymbol{\theta}^{[n]}$ are obtained via PMCMC and through it we also know the system dynamics and noise distributions which can be used to draw samples of both the processing noise $\boldsymbol{v}_{0:H}$ and measurement noise $\boldsymbol{w}_{0:H}$, which can be seen in the lines 4 and 5 of the Algorithm. Those samples can then be combined with the $\boldsymbol{x}_{\text{-}T:\text{-}1}$, or more precisely $\boldsymbol{x}_{\text{-}1}$ to find the initial state $\boldsymbol{x}_0$ to complete the scenario $\boldsymbol{\delta} = \{\boldsymbol{\theta}, \boldsymbol{x}_0, \boldsymbol{v}_{0:H}, \boldsymbol{w}_{0:H}\}$. How these scenarios can be used to find an optimal input $\boldsymbol{u}_{0:H}$ is described in the next section.

2.2 Chance-Constraint Optimization with Kernel Approximation

In the previous section, a method that enables us to generate a finite number of scenarios $\boldsymbol{\delta}^{[1:N]}$ was presented. These scenarios can be used to formulate an OCP to find an optimal $\boldsymbol{u}$ or a control law $\boldsymbol{\pi}$. In this section, a method to use maximum mean discrepancy (MMD) ambiguity sets and kernel approximation to reformulate the OCP is proposed.

2.2.1 MMD ambiguity sets

As the underlying data distribution P in the constraints (1.3) is unknown, we first expand the them to their distributionally robust counterpart in order to allow for the use of scenarios as an approximation of the distribution. For this, we consider P as the worst case distribution within a set $\mathcal{P}$ of plausible distributions, the so-called ambiguity set. This gives us the new constraints

$$\inf_{\tilde{P}\in\mathcal{P}} \tilde{P}\left[h(\boldsymbol{u}_{0:H}, \boldsymbol{x}_{0:H}, \boldsymbol{y}_{0:H}) \leq 0\right] \geq 1 - \alpha. \tag{2.1}$$

To construct the set $\mathcal{P}$, a similarity measure is needed to provide a concrete comparison between various distributions $\tilde{P}$. Maximum mean discrepancy (MMD) [GBR$^+$12] is able to do that by using the norm of the difference between the kernel mean embeddings (KME) $||\mu_Q - \mu_{Q'}||_{\mathcal{H}}^2$ of two distributions Q and Q' as a metric between two distributions. The KME are given as $\mu_Q = \int k(x, \cdot)\mathrm{d}x$ with $k(x, \cdot) \in \mathcal{H}$ being the feature map of the kernel function k. The metric can then be rewritten as

$$\mathrm{MMD}(Q, Q') = \mathrm{E}_{z,z'\sim Q}[k(z, z')] + \mathrm{E}_{z,z'\sim Q'}[k(z, z')] - 2\mathrm{E}_{z\sim Q, z'\sim Q'}[k(z, z')] \tag{2.2}$$

The MMD-based ambiguity set $\mathcal{P}$ is then constructed as the set of distributions $\tilde{P}$ in an ε radius centered around the empirical distribution P_N which is given through the scenarios $\boldsymbol{\delta}^{[1:N]}$. This gives us the set

$$\mathcal{P} = \{P : \mathrm{MMD}(P, P_N) \leq \varepsilon\}. \tag{2.3}$$

The radius ε is chosen through constructing a bootstrap MMD ambiguity set as described in [NKSZ22] and is outlined in Algorithm 2. This procedure requires a number of bootstrap samples B to be chosen, as well as confidence level β. It then utilizes kernels $k(\boldsymbol{\delta}^{[i]}, \boldsymbol{\delta}^{[j]}) \in \mathbb{R}$ to define the (biased) MMD estimator as

$$\widehat{\mathrm{MMD}}(\tilde{P}, P_N) = \sum_{i,j=1}^{N} k(\boldsymbol{\delta}^{[i]}, \boldsymbol{\delta}^{[j]}) + k(\tilde{\boldsymbol{\delta}}^{[i]}, \tilde{\boldsymbol{\delta}}^{[j]}) - 2k(\boldsymbol{\delta}^{[i]}, \tilde{\boldsymbol{\delta}}^{[j]}) \tag{2.4}$$

with $\tilde{\boldsymbol{\delta}}^{[n]}, n = 1, ..., N$, denoting a bootstrap sample of P_N where samples are drawn with replacement from $\boldsymbol{\delta}^{[1:N]}$. Finally, $\widehat{\mathrm{MMD}}(\tilde{P}, P_N)$ is calculated for all B bootstrap samples, the results are saved in list and ε is chosen as the $ceil(B\beta)$-th element of the sorted list.

2.2.2 Constraint Reformulation

With a given MMD ambiguity set $\mathcal{P}$, the feasible set of each constraint 1.4 is given as

$$Z_i := \left\{\boldsymbol{u}_{0:H} \in \mathcal{U}^{H+1} : \inf_{P\in\mathcal{P}} P\left[\tilde{h}_i(\boldsymbol{u}_{0:H}, \boldsymbol{\delta}) \leq 0\right] \geq 1 - \alpha\right\}. \tag{2.5}$$

with $\tilde{h}_i(\boldsymbol{u}_{0:H}, \boldsymbol{\delta}) = h_i(\boldsymbol{u}_{0:H}, \boldsymbol{x}_{0:H}, \boldsymbol{y}_{0:H})$.
We can now use the ambiguity set $\mathcal{P}$ defined in Sec. 2.2.1 with the radius ε and the kernel matrix $\boldsymbol{K}$ to reformulate the feasible set. The matrix $\boldsymbol{K}$ contains the kernels of all possible combinations of samples. By following the steps described in [NKSZ22], we can obtain the new reformulated feasible set as

---

Algorithm 2 Bootstrap MMD ambiguity set

   Input: Scenarios $\boldsymbol{\delta}^{[1:N]}$, Number of bootstrap samples B, Confidence level β
   Output: Gram matrix $\boldsymbol{K}$, Radius of MMD ambiguity set ε

1: $\boldsymbol{K} \leftarrow kernel(\boldsymbol{\delta}, \boldsymbol{\delta})$
2: **for** $m = 1, \ldots, B$ **do**
3:     $I \leftarrow N$ numbers from $\{1, \ldots N\}$ with replacement
4:     $K_x \leftarrow \sum_{i,j=1}^{N} K_{ij}$;
5:     $K_y \leftarrow \sum_{i,j \in I} K_{ij}$;
6:     $K_{xy} \leftarrow \sum_{j \in I} \sum_{i=1}^{N} K_{ij}$;
7:     $\text{MMD}[m] \leftarrow \frac{1}{N^2} \left(K_x + K_y - 2K_{xy} \right)$;
8: **end for**
9: $\text{MMD} \leftarrow sort(\text{MMD})$
10: $\varepsilon \leftarrow \text{MMD}[ceil(B\beta)]$

$$
Z_i := \left\{ \boldsymbol{u}_{0:H} \in \mathcal{U}^{H+1} : \begin{array}{ll} g_0 + \dfrac{1}{N} \sum_{n=1}^{N} (\boldsymbol{K}\boldsymbol{\gamma})_n + \varepsilon \sqrt{\boldsymbol{\gamma}^{\mathrm{T}} \boldsymbol{K}\boldsymbol{\gamma}} \le t\alpha & \text{(2.6a)} \\[3mm] [\tilde{h}_i(\boldsymbol{u}_{0:H}, \boldsymbol{\delta}^{[n]}) + t]_+ \le g_0 + (\boldsymbol{K}\boldsymbol{\gamma})_n, \ n = 1, ..., N & \text{(2.6b)} \\[3mm] g_0 \in \mathbb{R}, \boldsymbol{\gamma} \in \mathbb{R}^N, t \in \mathbb{R} & \text{(2.6c)} \end{array} \right\}
$$

where $[\cdot]_+ = \max(0, \cdot)$ denotes the max operator. The new set also contains new variables that have to be taken into account when solving the OCP. The variables g_0, γ and t are additional degrees of freedom can be incorperated into the OCP. The former are parameters of the RKHS function that was used to transform the problem into a kernel machine learning problem while t has been introduced as a way to relax the risk factor α.

This approximation can then be repeated for all other constraints $\boldsymbol{h}(\cdot)$ to obtrain the feasible sets $Z_i, i = 1, ..., n_c$. We can then use those constraints to formulate the OCP as

$$
\min_{\boldsymbol{u}_{0:H}, \{\boldsymbol{\gamma}, g_0, t'\}^{[1:n_c]}} J_H(\boldsymbol{u}_{0:H}) \tag{2.7a}
$$

$$
\text{s.t. } \forall n = 1, ..., N, \ \forall t = 0, 1, ..., H, \ \forall i = 1, ..., n_c \tag{2.7b}
$$

$$
\boldsymbol{x}_{t+1}^{[n]} = \boldsymbol{f}_{\boldsymbol{\theta}^{[n]}} \left(\boldsymbol{x}_t^{[n]}, \boldsymbol{u}_t \right) + \boldsymbol{v}_t^{[n]} \tag{2.7c}
$$

$$
\boldsymbol{y}_t = \boldsymbol{g}_{\boldsymbol{\theta}^{[n]}} \left(\boldsymbol{x}_t^{[n]}, \boldsymbol{u}_t \right) + \boldsymbol{w}_t^{[n]} \tag{2.7d}
$$

$$
\boldsymbol{u}_{0:H} \in Z_i(\boldsymbol{\gamma}^{[i]}, g_0^{[i]}, t'^{[i]}) \tag{2.7e}
$$

As described in Sec. 1.1, we are minimizing a cost function J_H. The system dynamics are included through the constraints (2.7c) and (2.7d) and must be fulfilled for all scenarios as well. Lastly, the input $u_{0:H}$ is restricted to the feasible sets Z_i, i.e. $u_{0:H}$ must be an element of all $Z_i, i = 1, ..., n_c$.

The optimization problem (2.7) is deterministic and can be solved with well known methods.

Chapter 3

Evaluation

In this section, the effectiveness of the proposed optimal control approach is tested in a simulation and compared it to previously used scenario theory. The simulation setup is described in section 3.1. The results of the OCP are shown in Sec. 3.2. Afterwards, we analyse the results and performance in more detail in section 3.3 by looking at the robustness of the solution and compare it to the commonly used scenario approach.

3.1 Simulation Setup

We consider a system with the state transition function

$$\boldsymbol{f}(\boldsymbol{x}, u) = \begin{bmatrix} 0.8x_1 - 0.5x_2 \\ 0.4x_1 + 0.5x_2 + u \end{bmatrix} \tag{3.1}$$

and the process noise distribution

$$\boldsymbol{v}_t \sim \mathcal{N}\left(\boldsymbol{0}, \begin{bmatrix} 0.03 & \text{-}0.004 \\ \text{-}0.004 & 0.01 \end{bmatrix}\right). \tag{3.2}$$

Both the state transition function and the process noise distribution are unknown to the user. Meanwhile, the observation function $g(\boldsymbol{x}, u) = x_1$ and measurement noise $w_t \sim \mathcal{N}(0, 0.1)$ is assumed to be known. This assumption can be made without a loss of genrality since an unknown observation model can be combined with the unknown transition model into a expanded model with $n_x + n_y$ states [Fri15].

For the scenario generation, we consider a set containing $T = 2000$ input and output measurements of the true system for our dataset $\mathbb{D}$. These measurements are obtained with a random input trajectory $u \sim \mathcal{N}(0, 3)$ while starting from a random initial state $\boldsymbol{x}_{\text{-}T} \sim \mathcal{N}([2, 2]^{\mathrm{T}}, \boldsymbol{I}_2)$. To infer the state model parameters, the approach from [AS17] is used. It is assumed that $\boldsymbol{f}(\cdot)$ is a linear combination of n_a basis functions $\boldsymbol{\varphi}(\boldsymbol{x}_t, u_t)$ and the process noise is normally distributed. As such, the state transition can be rewritten as

$$\boldsymbol{x}_{t+1} = \boldsymbol{A}\boldsymbol{\varphi}(\boldsymbol{x}_t, u_t) + \boldsymbol{v}_t \tag{3.3}$$

with the basis functions $\boldsymbol{\varphi}(\boldsymbol{x}, u) = [x_1, x_2, u]^{\mathrm{T}}$, the process noise $\boldsymbol{v}_t \sim \mathcal{N}(\boldsymbol{0}, \boldsymbol{Q})$ and the unknown parameters $\boldsymbol{\theta}$ consisting of $\boldsymbol{A}$ and $\boldsymbol{Q}$. An inverse Wishart prior with l degrees of freedom and positive definite scale matrix Λ is assumed for the matrix $\boldsymbol{Q}$. For the matrix $\boldsymbol{A}$ matrix normal prior with mean matrix $\boldsymbol{M} = \boldsymbol{0}$, right covariance $\boldsymbol{U} = \boldsymbol{Q}$ and left covariance matrix $\boldsymbol{V} \in \mathbb{R}^{n_a \times n_a}$. For the estimation of the posterior disdribution with the PG sampler, we scale the basisvector with the weights $[0.1, 0.1, 1]^{\mathrm{T}}$ and for the prior the weights are chosen as $\boldsymbol{V} = 10\boldsymbol{I}_5$.

We use gaussian kernels $k(x, y) = \exp\left(-\frac{1}{2\sigma^2}||x - y||_2^2\right)$ with the bandwidth σ set individually for all random parameters $\left\{\boldsymbol{x}_0^{[k]}, \boldsymbol{v}_{0:H}^{[k]}, w_{0:H}^{[k]}, \boldsymbol{A}^{[k]}\right\}$. As such, the elements of the Gram matrix $\boldsymbol{K} \in \mathbb{R}^{N \times N}$ are defined as

$$K_{ij} = k_{\sigma_A}(\boldsymbol{A}^{[i]}, \boldsymbol{A}^{[j]})k_{\sigma_\mathcal{X}}(\boldsymbol{x}_0^{[i]}, \boldsymbol{x}_0^{[j]})k_{\sigma_\mathcal{V}}(\boldsymbol{v}_{0:H}^{[i]}, \boldsymbol{v}_{0:H}^{[j]})k_{\sigma_\mathcal{W}}(\boldsymbol{w}_{0:H}^{[i]}, \boldsymbol{w}_{0:H}^{[j]}). \tag{3.4}$$

The individual elements of $\boldsymbol{\sigma} = [\sigma_A, \sigma_\mathcal{X}, \sigma_\mathcal{V}, \sigma_\mathcal{W}]$ are initialized via the median heuristic [GJK18] and then scaled to maximize the average probability of a set of N_{test} test samples, i.e. find the $\boldsymbol{\sigma}$ that maximizes

$$\max_{\sigma} \frac{1}{N_{\text{test}}} \sum_{n=1}^{N_{\text{test}}} \mathrm{P}_{\boldsymbol{\sigma}}(\boldsymbol{\delta}_{\text{test}}^{[n]}) \tag{3.5}$$

with the probability function being the product of the four Gaussian probability functions

$$\mathrm{P}_{\boldsymbol{\sigma}}(\boldsymbol{\delta}_{\text{test}}^{[n]}) = \prod_{\sigma_i \in \boldsymbol{\sigma}} \frac{1}{N_{\text{train}}} \sum_{m=1}^{N_{\text{train}}} \frac{1}{\sqrt{2\pi\sigma_i^2}} k_{\sigma_i}(\boldsymbol{\delta}_{\text{train}}^{[m]}, \boldsymbol{\delta}_{\text{test}}^{[n]}) \tag{3.6}$$

over a set of N_{train} training samples that are independent of the set N_{test}.

3.2   Optimal Control with Constrained Output

In the following, we show how well the proposed optimal control approach works when applied to a OCP with constrained output by putting it side by side with the solution of the same problem where we have used the scenario approach which implements the chance-constraints by ensuring that the constraints are satisfied for every scenario $n \in \mathbb{N}_{\leq N}$ [SG22].

For this simulation, we are using scenarios that have been generated using the PG sampler. To this end, 16130 samples were created and the first $N_p = 2000$ were discarded as training samples and the remaining samples were once again thinned with $n_d = 70$. The remaining $N = 200$ samples are then used as scenarios for the OCPs.

For the cost function, we consider a simple quadratic cost $J_H = \sum_{t=0}^{H} u_t^2$ over the horizon $H = 40$. For constraints, we consider the input-constraint $|u| \leq 10$ as well as the temporarily active output-constraints $y_{10:20} \leq -10$ and $10 \leq y_{30:40}$. ε is chosen through Algorithm 2 with a number of bootstrap samples $B = 1000$ and a confidence level $\beta = 0.95$. In this experiment, we look at the results for the risk level α being chosen as 0.01, 0.2 and 0.5 to determine how much of an influence this parameter has on the solution.

The OCP can then be formulated as described in section 2.2.2. Since the problem has been chosen as convex in this example, a solution for both the scenario and kernel approach can be found easily by using a convex solver.
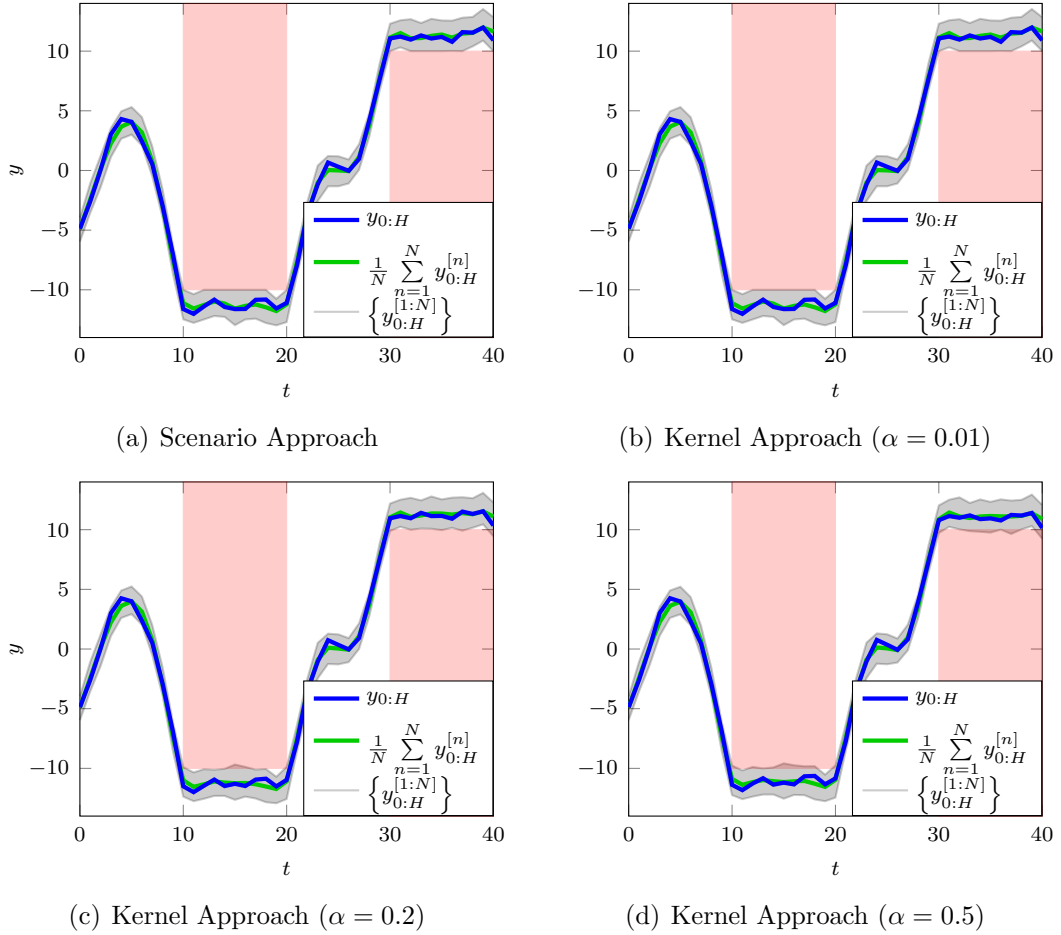

(a) Scenario Approach

(b) Kernel Approach ($\alpha = 0.01$)

(c) Kernel Approach ($\alpha = 0.2$)

(d) Kernel Approach ($\alpha = 0.5$)

Figure 3.1: Example of the optimal control with known basis functions for scenario approach (top left) and kernel approach for various values of α. The red areas show the output constraints. The gray area encompasses the 200 scenarios that were used in the optimization with the green line being the average. The blue line is one realization of the true output.

The results of an exemplary run is shown in Fig. 3.1. The figure includes the four

plots for the scenario and kernel approach for each α and shows the output y of their respective OCPs. The graphs shows the spread of the $N = 200$ trajectories that are generated when the input $\boldsymbol{u}_{0:H}$ is applied to the scenarios that were used to find the optimal input. On top that, it also shows of the mean of these trajectories and true output. Where the two graphs differ however is to what extend the solutions fulfill the constraints. By its definition, the scenario approach requires all scenarios to fulfill the constraints which can be seen in the solution. While the gray area touches the lower and upper bounds during several timesteps, it never violates the constraints. The kernel approach on the other hand has a risk factor α built in which allows for a number of scenarios to violate the constraints as long a sufficient number satisfies them. This can be seen in the constraint still being met by the majority of the scenarios and only the trajectory of a small number of scenarios actively overlapping with the marked area. This is especially apparent in the plots with larger α values. In contrast, the graph where α is chosen as 0.01 is almost identical to the scenario approach. These results show that the kernel approach allows us to find solutions outside the feasible region of the scenario approach and potentially find a solution with a lower cost. This is done in exchange for an increased risk of the true output violating one or more of the constraints which can be seen by the blue line being closer to the constraints. A particularly close example can be seen at $t = 40$ being where the true output comes very close to the constraints for $\alpha = 0.5$ but stays further away for the scenario approach or $\alpha = 0.01$.

3.3   Robustness

The biggest advantage that this kernel approximation has shown compared to the scenario approach is the adjustable risk factor. As described in Sec. 2.2, this method includes a parameter $\alpha \in [0, 1]$ which can be chosen depending on how successful the final solution is supposed to be when it comes to satisfying the constraints in future scenarios.

In this section, this parameter is tested by running the same problem setup as was used in Sec. 3.2 for different values of α as well as increasing and lowering the number of samples N and testing how well the solution holds up for other scenarios that are independent of the ones used in the optimization.

Similar to Sec. 3.2, a number of scenarios are generated with Algorithm 1. From this set of scenarios, a small subset is then taken and used to formulate several OCPs as was already described in Sec. 3.2. The OCPs are then solved and the resulting optimal input $\boldsymbol{u}_{0:H}$ is applied to $N = 2000$ more independent scenarios from the same system to test how well this solution holds up. For each of the 2000 scenarios, the output is calculated and compared to the constraints that were used in the OCP to check whether or not they are fulfilled. This process is then repeated for various numbers of scenarios. It is done for 1, 5, 10, 25 and 50 samples and then increased with a step size of 50 until $N = 300$ samples are used in the optimization.
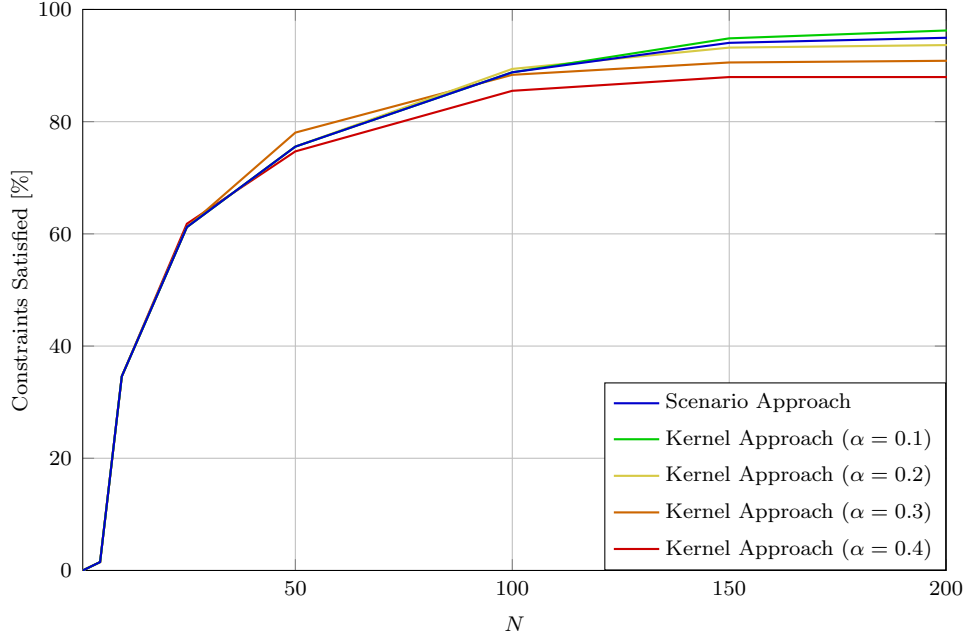
Figure 3.2: Percentage of scenarios where $u_{0:H}$ is a feasible solution. The blue line shows the result of the scenario approach while the other lines are for the kernel approach with various values of α.

In Fig. 3.2 the results of this simulation are shown. The percentage of scenarios that fulfill the constraints is plotted over the number of samples used in the initial optimization which range from $N = 1$ to 300. The various α values are shown as separate lines. Initially, all five plots show very similar results. This can be explained by the fact that at such a low number of scenarios cannot accurately represent the distribution. As the number of scenarios is increased, the approximation of the distribution becomes better leading to a higher percentage of scenarios where the constraints are satisfied.

After around 25 scenarios, the plots start diverging for the first time. While the scenario approach and the plots with smaller α values are very similar, the lines that represent larger α values are starting to display a slightly different percentage of cases that satisfy the constraints. It can be seen that the kernel approach achieves a more robust solution for $\alpha = 0.3$ and $N = 50$ but since this effect is only present for this one timestep, it can be inferred that this is most likely just due to random chance.

For $N \geq 100$ scenarios, a trend starts to become apparent in the different lines as all of them start to slowly converge with the risk factor α determining to what percentage each line converges. An interesting oddity that can be seen here is that the 3 lines for $\alpha = 0.2, 0.3$ and 0.3 all display the same pattern of their percentage increasing slighly above the rest of the curves before they drop below the rest. After that, the lines converge to various values that are dependent on the value α that's associated with each line.

Meanwhile, the scenario approach is displaying a similar be
While the scenario approach keeps increasing, the kernel approach seems to converge to a significantly lower level of robustness based on the selection of the parameter α. This shows that through α we are able to control how distributionally robust the solution is.

As the number of scenarios used in the optimization keeps increasing, first signs of their behavior for $N \to \infty$ become visible. While we require more samples to be sure of the exact percentages the approaches are converging to, it is already clear that they are not converging towards $(1 - \alpha)$ as we has hoped. For example, the line for the kernel approach with $\alpha = 0.2$ does not converge to 80% but instead a value around 50%. It can also be shown that this percentage is highly dependent on the number and types of constraints used. That is because the way the constraints are set up does not lend itself to precisely controlling the ratio between cases that satisfy all of the constraints and cases that violate one or more of them. This can potentially be solved by replacing the n_c constraints with a single one of the form $\max(\boldsymbol{h}(\cdot)) \leq 0$ which will require further testing in the future.

3.4   Corridor Test

(a) Scenario Approach

(b) Kernel Approach ($\alpha = 0.1$)

(c) Kernel Approach ($\alpha = 0.2$)
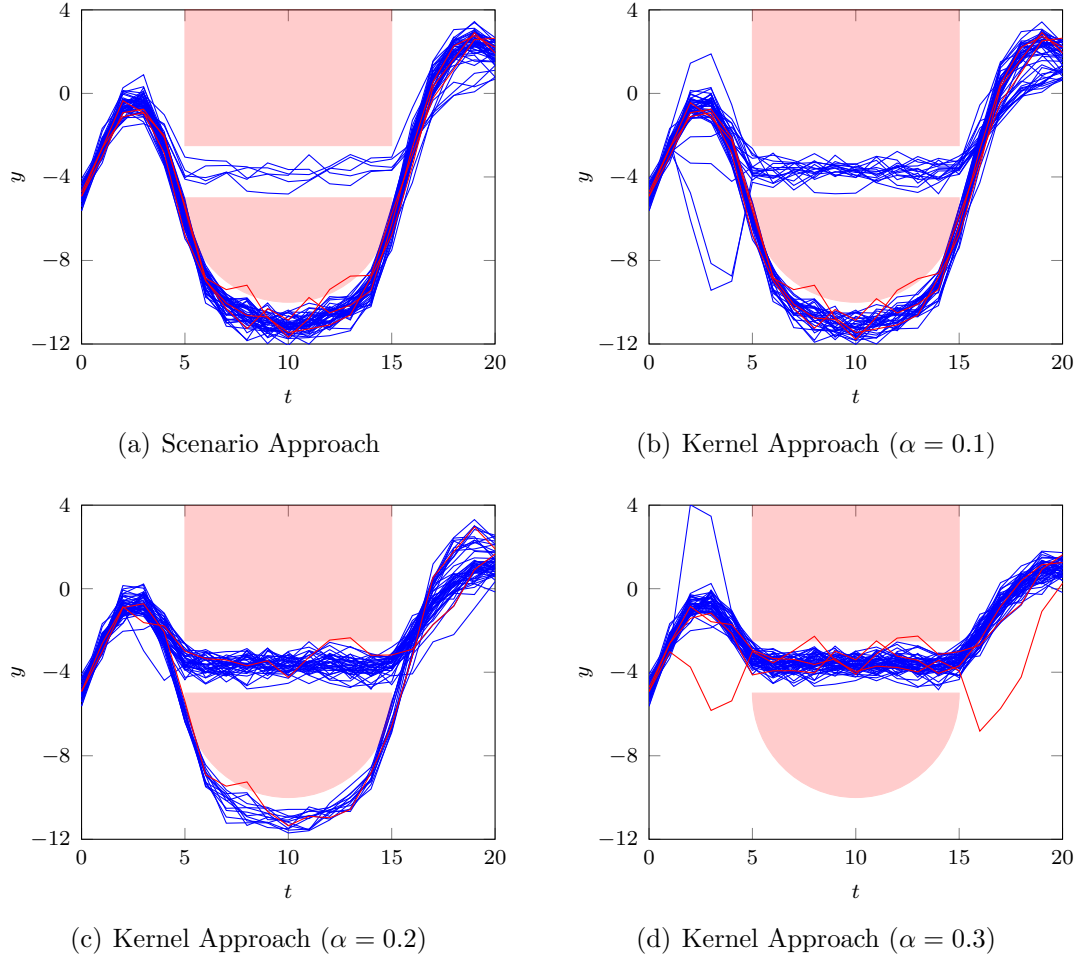
(d) Kernel Approach ($\alpha = 0.3$)

Figure 3.3: Example of the optimal control with known basis functions for scenario approach (top left) and kernel approach. The red areas show the output constraints. The lines show trajectories of the true system. The outputs that successfully avoid the constraints are colored blue, while all the outputs that violate at least one constraint are colored red.

Chapter 4

Discussion

Chapter 5

Conclusion

This work presented an alternate approach to scenario theory for the use of samples generated using PMCMC methods. The samples are drawn from the persterior distribution for the trajectories of an unknown system using a PG sampler and then used to define MMD ambiguity sets with the use of kernel embeddings. These sets are then used to reformulate a chance-constrained OCP while including a parameter for the permitted failure probability. This problem can then be solved used well-known methods.

The viability of this approach has been shown in several simulations where the methods were tested for an unknown linear system with a constrained output. The predicted output has been plotted and compared with the real output for the OCPs that were generated using scenario theory and MMD ambiguity sets. The effect of the permitted failure probability has also been shown for various numbers of scenarios being used when formulating the OCP. These results have demonstrated that the failure percentage is not converging to the selected parameter. Future work will investigate the cause of this and also try to expand the linear systems to non-linear ones.

Bibliography

[ADH10]   Christophe Andrieu, Arnaud Doucet, and Roman Holenstein. Particle Markov chain Monte Carlo methods. *Journal of the Royal Statistical Society: Series B (Statistical Methodology)*, 72(3):269–342, 2010.

[AS17]   Thomas Schoen Andreas Svensson. A flexible state-space model for learning nonlinear dynamical systems. *Automatica*, 80:189–199, 2017.

[Fri15]   Roger Frigola. Bayesian time series learning with Gaussian processes. *Ph.D. dissertation, University of Cambridge*, 2015.

[GBR+12] Arthur Gretton, Karsten Borgwardt, Malte Rasch, Bernhard Scholkopf, and Alexander Smola. A Kernel Two-Sample Test. *Journal of Machine Learning Research 13*, 2012.

[GJK18]   Damien Garreau, Wittawat Jitkrittum, and Motonobu Kanagawa. Large Sample Analysis of the Median Heuristic. *arXiv:1707.07269*, 2018.

[HCL19]   Ashish R Hota, Ashish Cherukuri, and John Lygeros. Data-Driven Chance Constrained Optimization under Wasserstein Ambiguity Sets. *American Control Conference (ACC)*, 2019.

[LSLH24] Robert Lefringhausen, Supitsana Srithasan, Armin Lederer, and Sandra Hirche. Learning-Based Optimal Control with Performance Guarantees for Unknown Systems with Latent States. *European Control Conference*, 2024.

[NKSZ22] Yassine Nemmour, Heiner Kremer, Bernhard Schoelkopf, and Jia-Jie Zhu. Maximum Mean Discrepancy Distributionally Robust Nonlinear Chance-Constrained Optimization with Finite-Sample Guarantee. *arXiv preprint arXiv:2204.11564*, 2022.

[SG22]   Marco Campi Simone Garatti. Risk and Complexity in Scenario Optimization. *Mathematical Programming*, 191(1):243–279, 2022.

License

This work is licensed under the Creative Commons Attribution 3.0 Germany License. To view a copy of this license, visit http://creativecommons.org or send a letter to Creative Commons, 171 Second Street, Suite 300, San Francisco, California 94105, USA.